Springer

Journal of Mechanical Science and Technology 22 (2008) 2009~2015

Journal of Mechanical Science and Technology

www.springerlink.com/content/1738-494x
DOI 10.1007/s12206-008-0407-8

Wear behavior of diamond wheel for grinding optical connector ferrule - FEA and wear test - †

Chang-Min Suh[1,*], Kyo-Seouk Bae[1] and Min-Soo Suh[2]

[1]*School of Mechanical Engineering, Kyungpook National University 1370, Sankyuk-dong, Puk-ku, Daegu, 702-701, Korea*
[2]*School of Energy Science, Kyoto University, Gokasho Uji, Kyoto 611-0011, Japan*

(Manuscript Received June 26, 2007; Revised February 11, 2008; Accepted April 10, 2008)

Abstract

The grinding characteristics and the wear behavior of diamond wheel for grinding the optical connector ferrule were investigated by finite element analysis (FEA) and wear test. FEA of contact between diamond wheel and ferrule shows that the subsurface damage area of ferrule is 13μm from the interface of abrasive particle and matrix. Fallout of abrasive particle is affected by the stress state at the interface. A 2-D finite element model was established to calculate the distribution of stress at the interface. As the result of FEA, fallout condition of abrasive was concerned with the ratio of the critical protrusion; the ratio of particle size is about 0.6. FE model was established to investigate the effects of the diamond concentration of wheel. The FEA result shows that the lower concentration of it has larger wear volume due to the small stress propagation.. To investigate grinding performance, the pin-on-disc wear test was carried out for three types of concentrations 75%, 100% and 125%. Through the wear test, it was confirmed that the 75% wheel concentration has the highest amount of wear volume. This result shows good agreement with that of FEA. And 100% concentration by considering the grinding ratio of the wheel shows the best optimized result for the grinding performance.

Keywords: Ferrule; FEA (Finite Element Analysis); Diamond wheel; Wear; Pin-on-disc; Grinding

1. Introduction

Grinding with bound abrasives has been extensively used in forming and finishing components of many materials [1-5].The demand of parts associated with the advanced optical technology is increasing due to the growth and the expansion of the optical industry. Especially, super-precision optical parts associated with IT, NT and BT requires the high anti-deviation to accomplish the ultra precision machining.

The wear characteristics of ceramic materials and cutting tools are important factor to control the precision of the products, and it is widely studied by many researchers: e.g. mechanisms of material removal in grinding ceramics [6, 7], grinding of silicon nitride [8-10], energy concerns with grinding [11-14], and by relating the grinding forces and energy to various parameters associated with the nondeformed chip geometry [15, 16].

The understanding of the behavior of both the matrix and the diamond abrasives becomes important, due to the wide use of diamond tool [17-20]. The severe wear and/or fracture of the diamond wheel are a restriction to mass production; grinding process includes a sacrifice not only the workpiece but also the diamond wheel. The objective of this study is to investigate the wear characteristics of the ceramic ferrule grinding by the diamond wheel.

The FE method was used to analyze the stress distribution and the abrasive at the contact area of the ferrule. The wear test was performed to verify the FEA results and to find the optimal condition of grinding from the comparison of each results.

† This paper was recommended for publication in revised form by Associate Editor Maenghyo Cho

*Corresponding author. Tel.: +82 53 950 5573, Fax.: +82 53 950 6550
E-mail address: cmsuh@knu.ac.kr

2. Theoretical background

2.1 Cutting point spacing

The successive cutting point spacing and the contact arc length are necessary for creating the FE model by considering the concentration. First of all, the contact arc length, l_c, is formulated in kinematics of surface grinding, as shown in Eq. (1).

$$l_c = \left(1 + \frac{v}{V}\right)\sqrt{\frac{\Delta}{\frac{1}{D} + \frac{1}{d}}} \tag{1}$$

where, v: workpiece velocity [rpm] V: wheel velocity [rpm], Δ: cutting depth [μm], d: workpiece diameter [mm], D: wheel diameter [mm].

Theoretical successive cutting point spacing, a_{th} is calculated by Eq. (2).

$$a_{th} = \frac{2d_g}{3V_g} \tag{2}$$

where, d_g is an equivalent diameter [mm] when the abrasive is assumed as sphere, and V_g is the ratio of abrasive particle.

2.2 Grinding force for single abrasive

The Merchant's theory was used to evaluate the specific grinding energy of a single abrasive to create the FE model as a micro element of the grinding wheel. Fallout of an abrasive is mainly affected by tangential grinding force. The value of tangential grinding force was 2.31×10^{-4} [N]. This value was set up on the load condition of the FE model.

2.3 Grinding force acting on the abrasive

Shaw model [21] was used in this study. Applying the Shaw model to the FE model, the diamond shape particle was converted into the sphere which has a diameter of 20 μm and the frictional force was neglected. Tangential grinding force was considered as a direct relationship with the fallout of abrasives.

2.4 Specific wear rate and grinding ratio

Wear of the wheel is related to the amount of grinding. Inverse value of the specific wear rate is grinding ratio, G as shown in Eq. (3).

$$G = T/S \tag{3}$$

where, T is the wear volume of material, and S is the wear volume of wheel. The parameter G was evaluated to use as a standard of the economic efficiency of the diamond wheel.

3. Characteristics of materials

3.1 Characteristics of the zirconia ferrule

TZP (Tetragonal Zirconia Polycrystal) was used in this study as the test material. It has been using widely in broad industry because of the excellence in hardness, strength/weight ratio, thermal stability, and corrosion resistance.

3.2 Characteristics of the diamond wheel

Table 1 shows the material properties of a diamond and resin, which is the specification of the diamond wheel. In case of machining the ferrule, the diamond wheel which is made by a phenolic resin is used; it has relatively high elasticity but low grinding resistance. Phenolic resin can bring a high revolution and a high grinding amount due to a proper removing flash and scale. Generally the phenolic resin is used but fiber reinforced phenolic resin is also used in special demand. Elastic modulus of the diamond wheel applied in FE simulation was 46 GPa which was determined by an elastic modulus of grade N.

Table 1. Material properties and specification of the diamond wheel.

Properties	Diamond	Resin
Elastic Modulus (GPa)	1171	7
Poisson's ratio	0.1	0.3
Concentration	100%	
Mesh # (abrasive size)	#400(40μm)	
Grade	N (46 GPa)	
Outer diameter	60 mm	
Inner diameter	20 mm	
Thickness	5 mm	

4. Finite element analysis

4.1 Contact analysis between wheel and ferrule

4.1.1 Finite element model

The interacting surface, where the grinding area is minutely divided by 4-node rectangular plane of strain elements, is to generate the most accurate gradient for the stress which is large at this area.

Motion of the model was described as the wheel and ferrule has a relative rotations and the ferrule was fed into the wheel. In this analysis, the cutting depth was set as one tenth of the real cutting depth for analyzing the contact instantly. Time duration was set as 1 ms. During at 0.4 ms, the ferrule was moved in front of the diamond wheel, and during at another 0.3 ms, the grinding was processed. The rest of the time, the grinding process has ended. In this analysis, the stick-slip friction model was used at the interface of the wheel and ferrule.

4.1.2 Result of finite element analysis

Fig. 1 shows the stress variations at the interface between the wheel and ferrule for the depth from the contact point. Ferrule stress exceeded its own flexural strength, 1 GPa, after the contact duration at 0.1 ms. After this moment, the grinding process has been progressed rapidly by the fracture propagation of the ferrule.

Fig. 2 shows the distributions of the von Mises stresses between the wheel and ferrule for the depth from the contact point. The greatest amplitude of stress was generated on the contact point and decreased as the increase of its depth from the contact point. The stress reaches to the flexural strength under 100 μm depths from the contact point. The stress at the area, under about 63 μm depth from the surface, has exceeded its flexural strength of 1 GPa. The estimated subsurface damage was about 13 μm except for the cutting depth of 50 μm .

4.2 Interface analysis between abrasive and resin

4.2.1 Finite element model

Normal force and frictional force were generated by the relative motion of the abrasive and ferrule. These forces will generate the stress at the contact interface between abrasive and resin. This state of stress is determined by the load and wear amount of the abrasive [5]. Semi-infinite matrix model was created, which has 600 times larger size than real

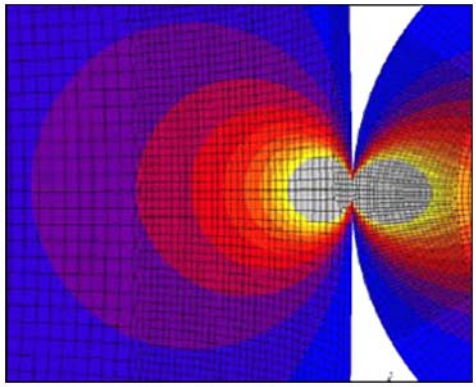

Fig. 1. Magnified distribution of von Mises stress at the contact interface.

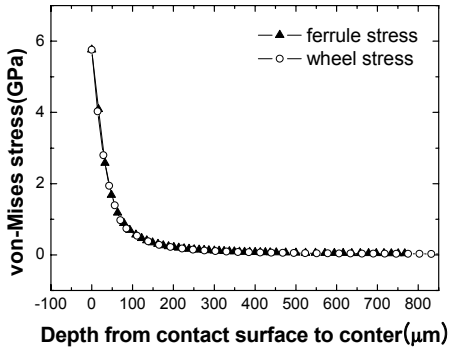

Fig. 2. Variation of von Mises stress of ferrule and wheel versus the depth from contact surface.

diamond abrasive. The stick-slip condition was selected as the boundary condition of the contact interface.

4.2.2 Finite element model for the wear mechanisms

Four types of assumptions for models were used as wear mechanisms in this analysis. No wear; a symmetric wear, the symmetrical wear before the diamond particle detached; an asymmetric wear which occurs only in one side around the resin of the diamond particle and the other side remains; and a particle wear which its amount of abrasive is relatively higher than that of resin.

4.2.3 Result of finite element analysis

Fig. 3 shows the stress distribution of all models. Fig. 3 (b) and (d) shows a state of moment just before the breakaway of the abrasive. The stress concentration occurred at the corner of the particle. The stress concentration has the greatest value, especially at the root of the particle. The stress concentration

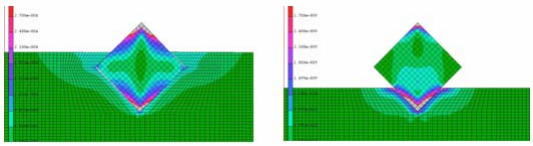

(a) No wear (b) Symmetric wear

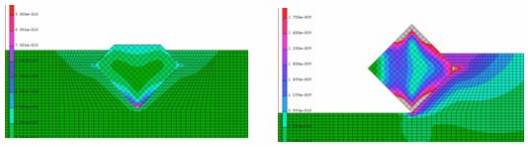

(c) Particle wear (d) Asymmetric wear

Fig. 3. Four kinds of stress distribution for the interface of abrasive and resin.

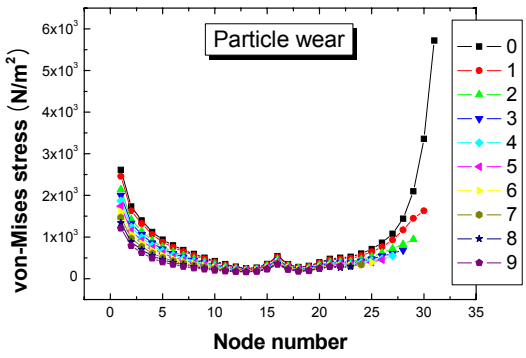

Fig. 4. Variation of von Mises stress versus node number as a function of particle wear.

was increased at the root of the particle as the wear progressed in both case of the wear, symmetric and the asymmetric. The stress at the interface of the resin and particle was higher than the stress at the particle tip, which directly applied to the grinding force. The ratio of the uncovered and covered part which led the breakaway of abrasive is about 0.6 and it corresponds with other paper [5].

Fig. 4 shows the stress distribution of the interface for nine cases of the particle wear. The characteristics of each specimen after and before the tests are listed in Table 2. The stress amplitude is three or four times larger than that of symmetric and asymmetric wear. The smaller stress of the interface between the abrasive and resin was, therefore, estimated at the root of the abrasive. In this case, it can be estimated that the wheel have to perform the dressing process.

Table 2. Grinding ratio and wear volume of the ferrule and diamond wheel.

nomenclature	Length of ferrule before test	Length of wheel after test	Wear volume of ferrule	Wear volume of wheel	Grinding ratio, G
1-1	10.47	7.81	52.18	0.62	80.03
1-2	10.47	6.27	82.40	0.83	98.84
1-3	10.48	7.95	49.63	0.50	99.49
2-1	10.48	7.33	61.80	0.77	80.24
2-2	10.46	6.38	80.04	0.73	109.54
2-3	10.45	7.57	56.50	0.63	89.38
3-1	10.46	6.93	69.25	0.76	91.15
3-2	10.46	6.13	84.95	0.68	125.73
3-3	10.46	7.78	52.58	0.58	94.21

Table 3. Three models of diamond concentration of wheel.

Concentration	V_g ;ratio of abrasive particle	a_{th}
75 %	0.1875	96.0
100 %	0.5200	72.0
125 %	0.3125	57.6

4.3 Analysis for the wheel concentration

4.3.1 Finite element model

The diamond concentration was used as a parameter for the evaluation. The grinding wheel consists of abrasive, resin and void. The role of void is to collect the chip; mainly affects on the discharge of the chip. Table 2 shows the successive cutting point spacing of the three different concentrations which was derived by the Eq. (2), and the ratio of the abrasive for the concentration of it. In each case, diamond concentration has the number of abrasive particles 75 % has 4; 100 % has 5; and 125 % has 6. Contact arc length, calculated by Eq. (1), was 374 μm and is applied to the model. There are two constraint conditions one is x direction at two side edges and the other is y direction at the bottom of the model.

4.3.2 Result of finite element analysis

The equivalent strain distribution of 100 % diamond concentration is shown in Fig. 5. The distributions of the strain are similar to the distributions of stress except for abrasives. The tensile side of the matrix, which applied the grinding force and the side edge, has a greater strain. This is caused by the stress concentration at the side edge. The larger the

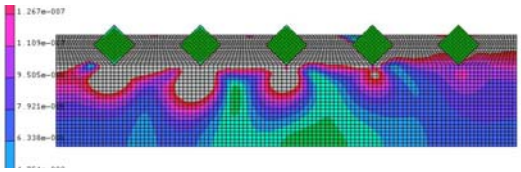

Fig. 5. An example of strain distribution according to the 100 % concentration of the diamond wheel.

concentration of the diamond is, the larger the strain occurs.

In case of the 75 % concentration, the border strain of the first particle was larger than the second one where the minimum value of the strain located closely. The phenomenon of 100 % concentration, similar to 125 %, was opposite to that of 75 % concentration. In case of the low concentration, the space among the particles was far from each other so that the influence among the particles hardly existed. Consequently, the strain of the first particle was relatively large and widely distributed due to the grinding force acting on the first diamond particle was larger than any other ones. In case of the 100 % concentration, the interaction between the first and second particle is not negligible because of the space among the particles was closer than that of 75 %.

Because of the influence among the abrasive particles, the strain has increased as the increase of concentration; the stress has decreased. The stress at the interface of the matrix and abrasive has relaxed according to the increase of the wheel concentration. It can be assumed that the factor of the abrasive fallout becomes weaken by the increase of the concentration.

5. Wear test

5.1 Result of wear test

The wear test of pin-on disc type was performed for diamond wheels which had different concentrations. The atmosphere was in-air temperature, no lubricated. The coefficient of friction was in the range of 0.44 to 0.46, in all test condition. In other words, it can verify that the unstable wear behavior has not occurred during the test.

Fig. 6 shows bar charts of the wear volumes of the ferrule and the diamond wheel. The wear volume of ferrule became large about 10 times rather than that of wheel. The wear volume of the 75 % concentration was the smallest one. The higher the diamond concentration is, the smaller wear of wheel occurs. In

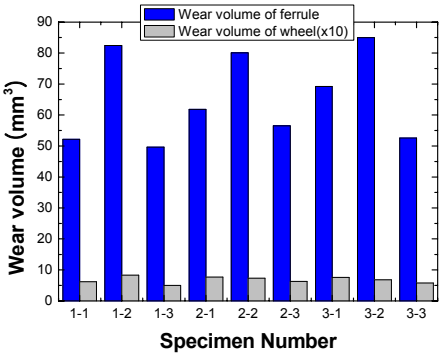

Fig. 6. Bar chart of the wear volumes of ferrule and wheel.

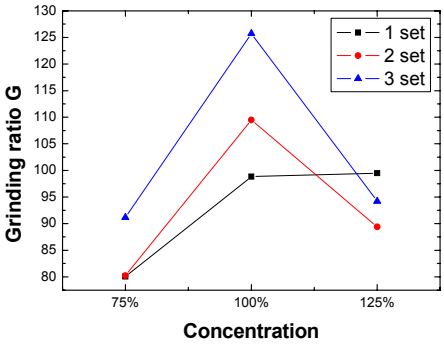

Fig. 7. Variation of grinding ratio, G versus concentration ratio.

case of the 100 % concentration, the ferrule has the largest wear volume. It looks like that the self-sharpening occurred but the glazing or loading has hardly occurred.

Fig. 7 shows the grinding ratio of each test set. In case of 100 %, it has the highest grinding ratio. In case of 75 %, on the other hand, it has the lowest grinding ratio. And in the case of 125 %, it was estimated to have the highest the grinding ratio due to the smallest wear volume.

5.2 Microscopic observation of wear surface

Fig. 8 shows SEM photography of the sectional view that diamond wheel of 75% concentration. A void, that many particles are shed in the resin, can be seen as V mark. A solid line indicates an interface of the surface and the section of the diamond wheel. The particle traces of breakaway can be observed.

In case of the 125 % concentration, the traces of the diamond (marked as D) of breakaway have not been observed, and the grinding face has a flat surface. If

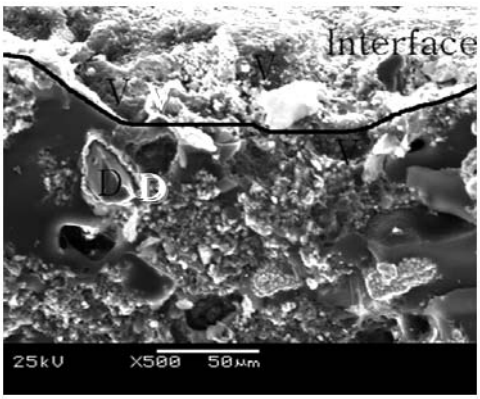

Fig. 8. SEM photography of 75 % concentration wheel (×500) shows voids(V) and diamond particles(D).

the grinding face becomes as the flat surface, the grinding resistance will be increased. And then, the wear occurs in the processing face of ferrule and wheel. Thus the quality of the ground face of ferrule becomes a low level.

6. Conclusions

The result of contact analysis shows that the area of subsurface damage becomes 13μm when the depth of cutting is 50 μm.

The result of interface analysis shows that the abrasive breakaway condition is the ratio of the critical protrusion; the breakaway of abrasive particle is about 0.6.

The result of FEA according to concentration ratio, the lower diamond concentration ratio has the higher stress concentration due to the lower interactive among the abrasives particles. Abrasive breakaway is, therefore, faster and the wear of the diamond wheel is propagated rapidly. These results are well corresponded with those of the wear test and also confirmed by the SEM observation.

The optimal condition of the diamond concentration ratio is 100 % and the worst condition of it is 75 %.

Acknowledgments

This research was supported by the Program for Training of Graduate Student in Regional Innovation which was conducted by the Korea Industrial Technology Foundation and the Ministry of Commerce, Industry and Energy of the Korean Government.

References

[1] Peter Blake, Thomas Bifano, Thomas Dow, Ronald O Scattergood, Precision Machining of Ceramic Materials, American Ceramic Society Bulletin 67 (6) (1988)1038-1041.

[2] S. Malkin and J. E. Ritter, Grinding Mechanisms and Strength Degradation for Ceramics, Journal of Engineering for Industry, (1989) 167-174.

[3] S. Malkin, Grinding Technology - Theory and Applications of Machining with Abrasives, Ch. I, Ellis Horwood, Chichester, (1989) 9-17.

[4] J. L. Mertzger, Super abrasive Grinding, Ch. 1, Butterworth, Oxford, (1986) 3-11.

[5] Y. Zhou, P. D. Funkenbusch and D. J. Quesnel, Stress Distribution at the Abrasives-matrix Interface during Tool Wear in Bound Abrasive Grinding-Finite Element Analysis, Wear 209 (1997) 247-254.

[6] Bi. Zhang, Howes and D. Trevor, Material-removal mechanisms in grinding ceramics, CIRP Annals - Manufacturing Technology 43 (1) (1994) 305-308.

[7] S. Malkin and T. W. Hwang, Grinding Mechanisms for Ceramics, Ann. CIRP, 45 (2) (1996) 569-580.

[8] T. W. Hwang, C. J. Evans and S. Malkin, Size effect for specific energy in grinding of silicon nitride, Wear 225-229 (PART II) (1999) 862-867.

[9] T. W. Hwang, C. J. Evans, E. P. Whitenton and S. Malkin, High speed grinding of silicon nitride with electroplated diamond wheels, part 1: Wear and wheel life, Journal of Manufacturing Science and Engineering, Transactions of the ASME 122 (1) (2000) 32-41.

[10] T. W. Hwang, C. J. Evans and S. Malkin, High Speed Grinding of Silicon Nitride With Electroplated Diamond Wheels, Part 2: Wheel Topography and Grinding Mechanisms, Journal of Manufacturing Science and Engineering, Transactions of the ASME 122 (1) (2000) 42-50.

[11] S. Malkin and N. Joseph, Minimum Energy in Abrasive Processes, Wear 32 (1), (1975) 15-23.

[12] T. W. Hwang and S. Malkin, Upper bound analysis for specific energy in grinding of ceramics, Wear 231 (2) (1999) 161-171.

[13] S. Malkin, Correlation between Solid Particle Erosion of Metals and Their Melting Energies, Wear 68 (3) (1981) 391-396.

[14] G. N. Shah, A. C. Bell and S. Malkin, Quantitative Characterization of Abrasive Surfaces Using a New

Profile Measuring System, Wear 41 (2) (1977) 315-325.
[15] C. Chen, Y. Jung and I. Inasaki, Surface, Cylindrical and Internal Grinding of Advanced Ceramics, Grinding Fundamentals and Applications, PED-Vol. 39, ASME (1989) 201-211.
[16] T. W. Hwang and S. Malkin, Grinding Mechanisms and Energy Balance for Ceramics, ASME J. Manuf. Sci. Eng., 121, (1999) 623-631.
[17] D. Miller and A. Ball, The wear of diamonds in impregnated diamond bit drilling, Wear 141 (1991) 311-320.
[18] Y. S. Uao and S. Y. Luo, Wear characteristics of sintered diamond composite during circular swing, Wear 157 (1992) 325-337.
[19] X. Tian and S. Tian, The wear mechanisms of impregnated diamond bits, Wear 177 (1994) 81-91.
[20] W. Konig and A. Neises, Wear mechanisms of ultrahard, non-metallic cutting materials, Wear 162/164 (1993) 12-21.
[21] M. C. Shaw, New Theory of Grinding, Inst Eng Aust. Mech. Chem. Eng Trans MC8 (1) (1972) 73-78.

Chang-Min Suh received his B.S. and M.S. degrees in mechanical engineering from Busan Na-tional University in 1964 and 1968, respectively, and received his Ph.D. degree from the University of Tokyo in 1981. He now is a professor at Kyungpook National University. He has served as the Head of the Department of Mechanical Engineering at Kyungpook National University, a Visiting Professor of Materials Science and Engineering in Univ. of California Berkeley, a Head of the Institute of Engineering Design Technology Kyungpook Nat'l Univ, and a Head of the Technology Innovation Center designated by the Department of Commerce and Industry of Korea.